AIAA SciTech Forum
6-10 January 2025, Orlando, FL
AIAA SCITECH 2025 Forum

10.2514/6.2025-0135

Comparison of Interfacial Delamination of Nanoparticle Modified Reinforcements in Functional Composites

Alexander Skoppe[1#], Yuxuan Wu[2#], Foram Madiyar[3] and Sirish Namilae[4*]
Embry-Riddle Aeronautical University, Daytona Beach, FL, 32114, USA

Nanoscale interface modification enables fiber reinforced composites to exhibit multifunctional behaviors in addition to enhancing fiber-matrix interface strength for improved load transfer. This study compares three distinct interfaces composing morphological nanoparticles: zinc oxide (ZnO) nanorods grown on carbon fibers (CF), manganese dioxide (MnO_2) nanowires grown on CF, and hydroxyapatite (HAP) nanocrystals grown on jute fibers (JF). Three hydrothermal growth procedures for fiber surface modification are presented. The adhesive properties of the interface are characterized through nanoscratch tests. The ZnO-CF interface presents the highest interfacial adhesion with an average magnitude of 3060 mN being required for fully peeling the ZnO coating off the fiber surface. Using the same analysis method, the HAP-JF interface possesses a relatively weaker interfacial adhesion which requires an average of 1360 mN to fully expose the jute fiber surface. The MnO_2-CF interface suggests the lowest interfacial adhesion which only requires an average force of 946 mN for a full fiber-coating delamination. Ultimately, this work characterizes and reveals the inherent variation of interfacial adhesion between the fiber substrate and nanoparticle coatings, which aims to provide valued insights for interface design in multifunctional composite applications.

I. Introduction

Fiber-reinforced composites represent a class of advanced materials where fiber reinforcements are specifically oriented in matrices such as polymeric materials. These composites offer enhanced performance and tailored attributes suited for diverse applications [1]. Synthetic carbon fiber reinforced composites (CFRCs) and natural fiber reinforced composites (NFRCs) represent two distinct classes of functional composites that have garnered significant attention in various industries due to their unique properties and applications. CFRCs, derived from petroleum-based precursors, boast exceptional strength-to-weight ratios, stiffness, and resistance to corrosion, making them ideal for aerospace and automotive applications [2]. In contrast, NFRCs utilize renewable resources such as plant fibers of bamboo, jute and hemp as reinforcement, offering biodegradability, lower energy consumption during manufacturing, and reduced environmental footprint [3].

The mechanical performance of CFRCs and NFRCs heavily relies on several key factors such as fiber mechanical properties, fiber orientation, fiber length, and fiber volume fraction [4]. Moreover, it is evident that the quality of interfacial adhesion between the fiber and the matrix is critical for transferring loads effectively and preventing fiber-matrix debonding or delamination [5]. Hence, interfacial modifications, such as chemical treatments using silane coupling agents, or physical treatments with plasma, are often induced to improve the fiber and matrix interaction and

---

[1] Doctoral Student, Aerospace Engineering
[2] Doctoral Student, Aerospace Engineering
[3] Assistant Professor, Physical Science
[4] Professor, Aerospace Engineering (Corresponding Author: namilaes@erau.edu)
[#] These authors contributed equally to this work.

subsequently enhance the interfacial bonding [6, 7]. Interfacial modification using nanoscale materials has been shown to enhance the properties of composites, as demonstrated by both computational models and experimental studies [8, 9]. Furthermore, nano-species interfacial modification has been proven effective to improve mechanical properties for both CFRPs and NFRPs. For instance, carbon fiber modified with ZnO nanorods and metal organic frameworks showed up to 18% increase in interfacial strength [9]. Jute fiber modified with hydroxyapatite nanoparticles exhibit 30 and 33% improvement in tensile strength and stiffness respectively [10].

While both CFRPs and NFRPs have reinforcing elements and load-transferring mechanisms, the interfacial interaction between the reinforcement and matrix of the two composites differ significantly due to the distinct properties of synthetic carbon fibers and natural fibers. For NFRCs, interfacial modification is often challenging due to the high hydrophilicity and biostochasticity of natural fibers, which are influenced by the plant growth processes and environmental conditions [11]. Interfacial modification of carbon fibers is often hindered by the nanomaterial agglomeration at fiber surface due to the high surface energy, leading to performance inconsistencies [12]. Moreover, the selection of nano-modifiers needs to address the potential effect on the matrix rheological properties where the curing kinematics of matrix material can be altered. These concerns established from varied fiber properties in CFRCs and NFRCs determine the modification process and necessitate the need for a comprehensive investigation of the interfacial adhesion obtained from various interfacial modifications. Understanding the interfacial interactions between various modifiers and underlying fiber substrates provides significant insight into functional composite design and manufacturing.

Nanoindentation techniques have been used for measuring the mechanical properties of bulk materials and have been further developed for evaluating the adhesion strength of coatings or films to the substrate [13, 14]. Specifically, a nanoscratch test is formulated based on an indentation perpendicular to the coating surface, where the applied load drives the indenter into the coating/substrate interface and induces a compressive radial stress in the coating, which provides the driving force for coating detachment [15]. Compared to the macroscale composite interfacial characterizations such as single-fiber pulling test, nanoscratch tests allow localized analysis at the fiber/modifier interface without the synergistic load contribution from matrix materials, accurate quantitative measurement such as critical delamination load, and repeatable damage-free characterizations with high sensitivity.

In this work, we investigate three types of nanomaterial functionalized composites and compare the delamination responses using nanoscratch tests. Firstly, we introduce the ZnO - carbon fiber adhesion for the application of high strength composites. It has been shown that growing ZnO nanorods onto the surface of the carbon fibers increases the interfacial strength significantly while not weakening the fibers [16]. In addition, it’s also been found that growing ZnO crystals on carbon fibers reduces the residual thermal stresses during processing [17]. Then, we investigate the MnO_2 - carbon fiber adhesion in electric composites applied as capacitors. MnO_2 is a polymorphic material, when it is grown in alpha-MnO_2 crystals it has a high specific capacitance. Further studies have found that carbon cloth, when modified with MnO_2 nanorods could be used as an electrode in super capacitors [18]. Furthermore, we investigate the hydroxyapatite (HAP) - jute fiber adhesion in insulating composites. Hydroxyapatite is a naturally-sourced biodegradable substance found in bones and tissues. The nanomaterials derived from HAP possess high stiffness, diverse morphologies, and offers a transition region from the hydrophilic jute fiber to the hydrophobic matrix while remaining the reinforcement biodegradability [19].

II. Experimentation

A. Interfacial Modification

We develop three distinct hydrothermal processes for carbon fibers and jute fibers. Three nano-modifiers, ZnO, MnO_2, and HAP, are grown onto the fibers at various conditions of temperatures and pressures. The hydrothermal growth processes are schematically depicted in Fig. 1. A scanning electron microscope (SEM) is utilized for microstructure analysis of nano-modifiers and the thickness of resulting coating layer. The modified fiber reinforcements are subsequently characterized for coating delamination using nanoscratch tests.

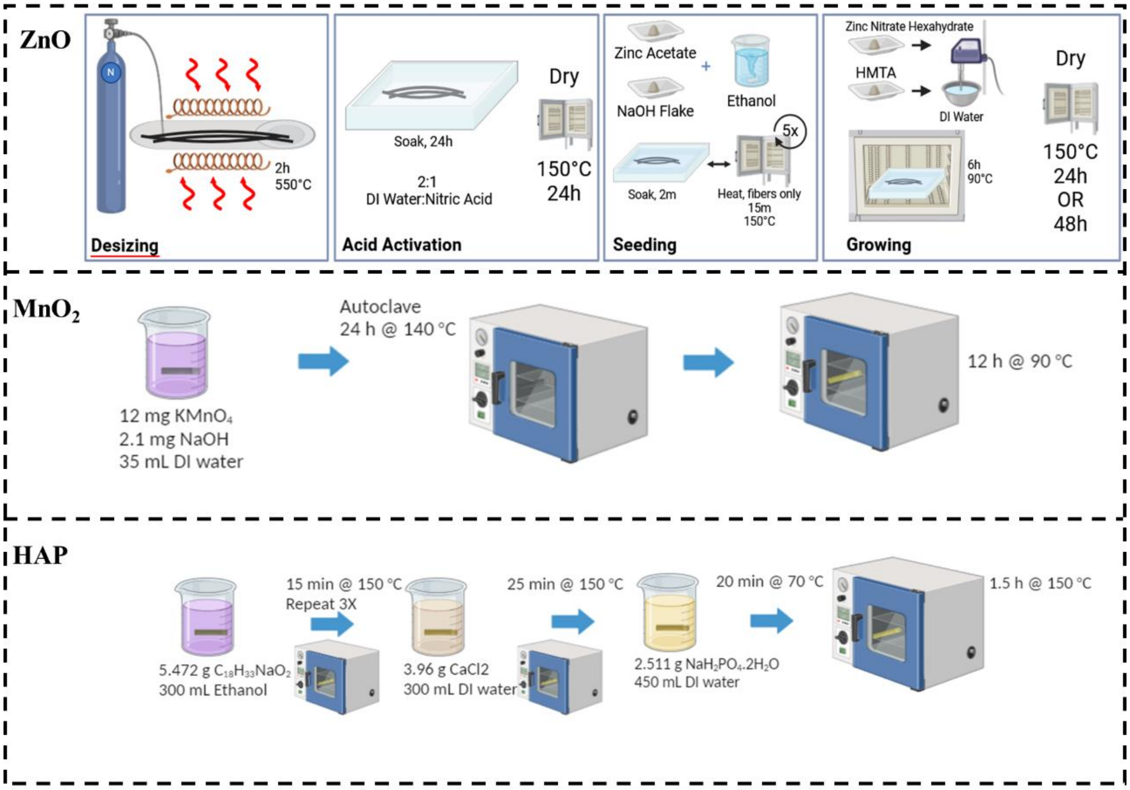

Fig. 1 Schematic diagrams of hydrothermal growth procedures.

B. Nanoscratch Testing

The interfacial adhesion characterization was conducted using a displacement sensing indentation (DSI) based Hysitron TI-980 triboindenter (Bruker Inc.), as shown in Fig. 2a. The adhesion characterization was performed using the displacement-controlled nanoscratch module of the nanoindenter equipped with a Berkovich tip, as shown in Fig. 2b. Despite that, the most commonly used type of tip for nanoscratch is the diamond conical Rockwell for thin coatings under 100nm, a sharp Bercovich tip can be used for coatings with the micrometer-scale thickness [20, 21]. The load function of each nanoscratch test contains three consecutive steps: indent, scratch, and lift, as shown in Fig. 2c. During the indenting stage, the probe was pressed down along the indenting axis perpendicular to the sample surface. After the piezo-transducer identified the tip at the sample surface, the probe was further controlled for a desired depth till the interface between the nano-modifier layer and the underlying substrate. During the subsequent scratch stage, the tip was maintained at the same depth but controlled for a movement along the scratch axis across the sample surface for a desired lateral displacement. During the lifting stage, the probe was lifted along the indenting axis while maintaining no movement along the scratch axis. Throughout all three stages, the responsive lateral forces were recorded for the interfacial adhesion analysis. The critical load ensuring the coating was fully peeled off corresponds to the adhesion strength [22].

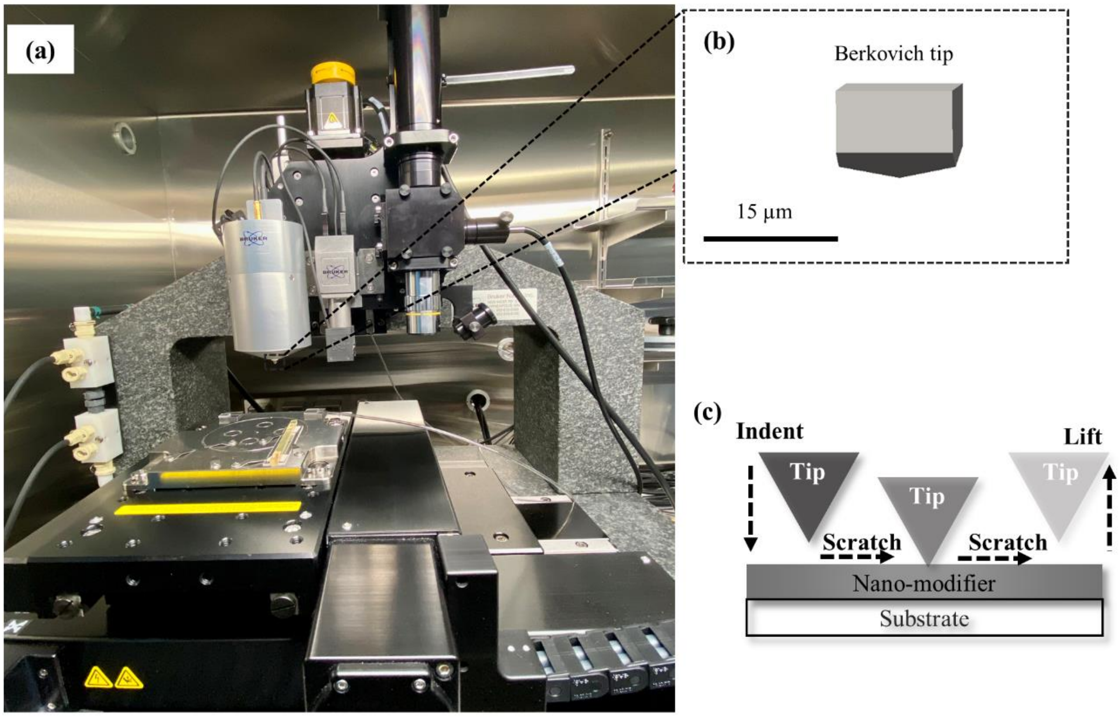

Fig. 2 Nanoscratch test setup. (a) Hysitron TI-980 triboindenter, and nanoscratch test setup. (b) Schematic depiction of Berkovich indentation tip. (c) Schematic depiction of nanoscratch coating delamination test.

For these scratch experiments, multiple measurements were taken to prevent the coating/substrate interfacial variations from having an effect on results. In each test, the load function was set up as follows. The depth of the indent was set according to the coating thickness measured from SEM microstructure analysis to guarantee the full peeling of at the substrate surface. The speed of the vertical component of the indent was kept at 0.5 µm/s. To avoid the accumulative resistance from the peeled-off coating substance, a distance of 10 µm was used as the scratch lateral displacement with a scratching rate of 0.67 µm/s. The same displacement and rate as the indenting was employed for the lifting stage as the final step.

III. Results and Discussion

A. Microstructural Characterization

Microstructural analysis using SEM suggested that the nanoparticles were strongly connected to the underlying fiber substrate with comprehensive coverage of the fiber. The representative microstructures are shown in Fig. 3. It can be seen from the SEM micrographs that each nanoparticle has a different morphology. As shown in Fig. 3a, ZnO nanorods generally have a hexagonal tubular shape that branches from the carbon fiber interface. Owing to the size of the ZnO nanorods, a porous layer was formed around the carbon fibers. Comparatively, Fig. 3b shows that the MnO_2 nanowires fill the area around the fiber more densely than the ZnO nanorods, resulting in a less porous surface. Fig. 3c shows that the HAP nanocrystals pattern the densest around the fiber surface, creating a surface with little porosity. Furthermore, the SEM micrographs revealed an average coating thickness of 2µm for all three types of modifiers. The coating thickness was calculated by comparing the SEM micrographs of unmodified fibers with those of the modified fibers and comparing the diameters of the fibers at five different locations.

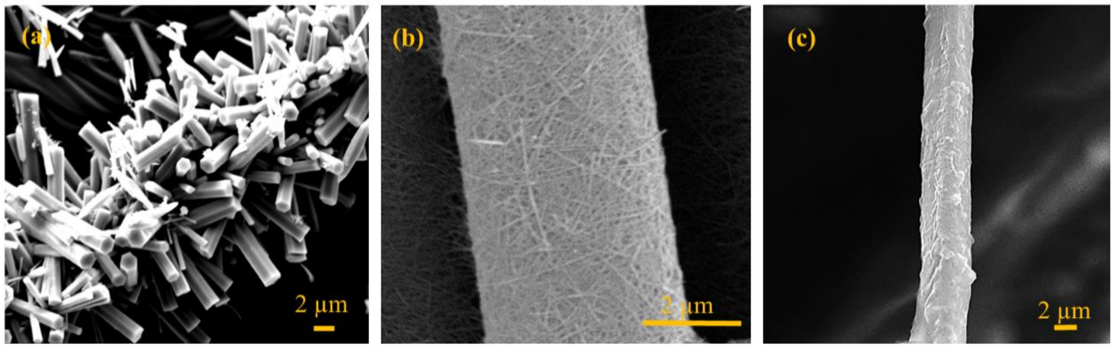

Fig. 3 Representative SEM microstructures of (a) ZnO nanorods, (b) MnO_2 nanorods, and (c) HAP nanocrystals.

B. Interfacial Adhesion Characterization

Firstly, Fig. 4 contains the reaction forces obtained through a representative nanoscratch test performed on ZnO-carbon fiber (CF) interface. The reaction force in the normal direction is shown in, Fig. 4a. It can be observed that, in the indent stage, the resistance initially increases as the tip indenting into the layer of ZnO nanorods. Once the tip reaching the desired depth of 2 μm, the normal force enters to a relatively steady state with an average magnitude of 1049 mN, indicating the isotropic resistance from the ZnO layer attributed from the stiffness of ZnO nanorods. As the tip is lifted away from the ZnO-CF interface, the stress is gradually released. Corresponding to Fig. 3a, reaction force obtained from the lateral scratch direction is shown in Fig. 4b. During the indenting stage, a slight decrease of lateral force is observed. This is likely due to the spatial rearrangement of ZnO nanorods. Due to the inherent high porosity of the ZnO layer, when in contact with the tip during the indenting stage, small amount of ZnO nanorods are fragmented before reaching the ZnO-CF interface. In the subsequent scratch stage, the lateral force remains at a relatively consistent level. The consistency of lateral force variation during the scratch stage suggests that a constant peel-off rate of ZnO nanorods from the CF surface with minimal accumulation of ZnO substances along the scratch direction. Moreover, the average force magnitude of 3042 mN in the lateral direction during the scratch stage is tightly related to the interfacial adhesion strength between the ZnO nanorods and CF substrate. Therefore, this feature of lateral force variation is adopted as a key metric for the subsequent comparison among three interfacial systems in this study. The statistical distribution of normal force and lateral force during the scratch stage obtained from the repeated test is shown in Fig. 4c, with an average magnitude and standard deviation of 1067 ± 140 mN and 3060 ± 160 mN, respectively.

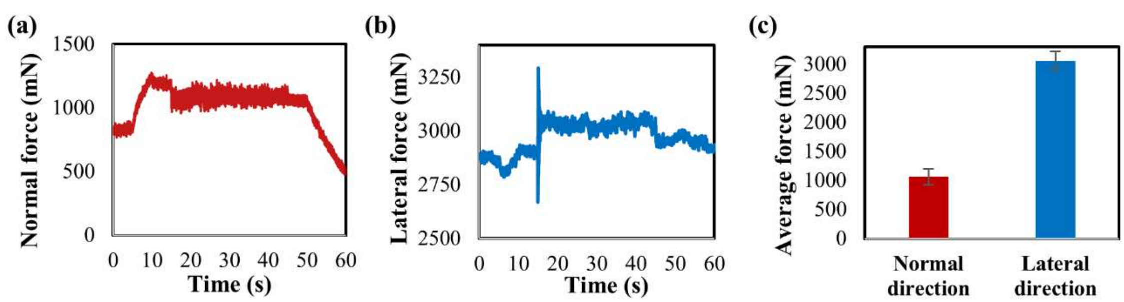

Fig. 4 Nanoscratch force responses of ZnO-CF in (a) normal direction along indenting axis and (b) lateral direction along the scratch axis.

Next, we investigate the adhesive behaviors of MnO_2/CF interfaces. The reaction forces obtained from a representative nanoscratch test is shown in Fig. 5. The normal force obtained from the MnO_2-CF interface is as shown in Fig. 5a. Similar to the behaviors observed from the ZnO-CF interfaces, the normal force slightly increases during the indenting stage. However, the magnitude of the normal force is overall higher than the normal forces obtained from the ZnO-CF surface. This is potentially attributed from the higher coverage density of the MnO_2 nanowires over the CF surface compared to the ZnO nanorods. The woven structure of the MnO_2 layer endows the interfacial region with higher resistance to the indenting tip. In the subsequent scratch stage, the normal force remains at a relatively consistent magnitude. Fig. 5b showcases the corresponding lateral force variation. During the scratch stage, the lateral force presents a lower average magnitude compared to the ZnO-CF interface. This indicates that the adhesion between the MnO_2 nanowires and CF substrate is not as strong as compared to the ZnO nanorods. Moreover, such explanation also addresses the slight increase of the lateral force and normal force during the scratch stage compared to the ZnO-CF interface. The tip is consistently subject to the increased resistance from the accumulation of peeled off MnO_2 nanowires. Similar to the analysis for ZnO-CF interface, the statistical distribution of normal force and lateral force during the scratch stage obtained from the repeated test is shown in Fig. 5c, with an average magnitude and standard deviation of 1340 ± 137 mN and 946 ± 110 mN, respectively.

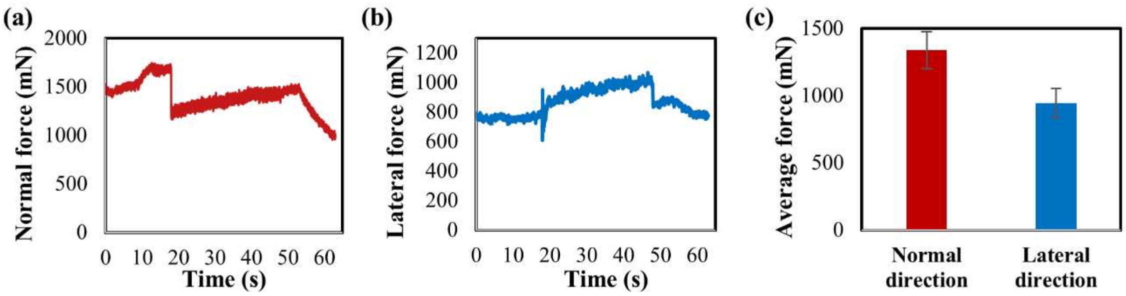

Fig. 5 Nanoscratch force responses of MnO2-CF in (a) normal direction along indenting axis and (b) lateral direction along the scratch axis.

Fig. 6 showcases the force responses obtained through nanoscratch tests performed on HAP modified jute fiber (JF). As shown in Fig. 6a, during the indent stage, the resistance initially increases as the tip indenting into the HAP layer. The magnitude of the normal force while approaching the HAP-JF interface is overall higher than both the interfaces of ZnO-CF and MnO_2-CF. This observation can be again explained by the higher filling density of HAP nanocrystals than the ZnO nanorods and MnO_2 nanowires. The HAP nanocrystals form a densely packed layer among the JF surface, which requires more efforts of the tip while approaching the HAP-JF interface. the lateral force from the corresponding representative test is shown in Fig. 6b. It can be observed that, at the initial stage of the scratch, the lateral force drastically increases to a consistent average magnitude of 1360 mN which indicates the interfacial adhesion of HAP nanocrystals and JF substrate. Such magnitude of lateral force obtained at the HAP-JF interface indicates a weaker adhesion than the ZnO-CF interface but stronger than the MnO_2-CF interface. Such observation is consistent among all the repeated test as shown in Fig. 6c. The average normal force and lateral force is measured for 2834 ± 109 mN and 1360 ± 95 mN, respectively.

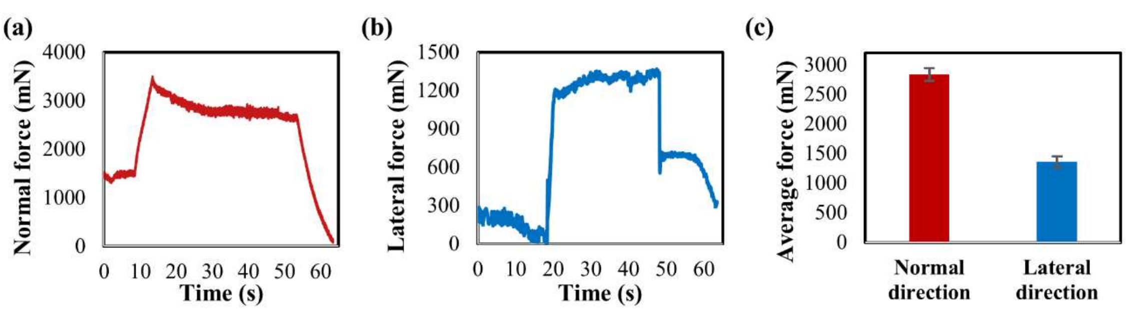

Fig. 6 Nanoscratch force responses of HAP - jute fiber in (a) normal direction along indenting axis and (b) lateral direction along the scratch axis.

Overall, it can be concluded that the morphology of the nanomaterial formed during fiber surface modification approaches has an effect on the overall stiffness on the interfacial region. This is evidenced by the normal forces obtained from the woven MnO_2 nanowires and highly agglomerated HAP nanocrystals compared to the individualized ZnO nanorods.

Comparing the magnitude of the reaction forces obtained from the lateral direction, a ranking of interfacial adhesion strength among three interfaces can be obtained. We note that, the ZnO-CF interface possesses the strongest adhesion, followed by the HAP-JF and the MnO_2-CF interface. This observation suggests implications for practical application of the three multifunctional composites. In addition to piezoelectric properties, ZnO nanowires impart the interfaces with the highest interfacial integrity for improved load transfer [17]. Therefore, ZnO enhancement can be used both for functional applications in structural health monitoring, and also to improve the mechanical properties in structural applications. In contrast, MnO_2 nanowires while enabling multifunctional applications such as super capacitors [23], may not significant improve the interfacial strength, therefore structural properties must rely primarily on carbon fibers. Similarly, considering the weak mechanical properties and unique structure of natural fibers, the interfacial strength inmprovement offered by HAP modification can expand the applications of NFR composites.

IV. Conclusions

In this study, we study and compare the interfacial delamination behaviors of nano-modified reinforcements in functional composites. Three interfacial systems composing ZnO nanorods with carbon fiber, MnO_2 nanowires with carbon fiber, and hydroxyapatite nanocrystals with jute fiber are investigated. We first utilize three hydrothermal growth approaches to formulate three distinct interfaces of interest. The microstructure analysis with SEM confirms the effective growth of the three nanospecies on the corresponding fiber substrate. We then use nanoscratch tests to measure the interfacial adhesion existing in the three interfaces. The ZnO-CF interface presents the highest interfacial adhesion with an average magnitude of 3060 mN being required for fully peeling the ZnO coating off the fiber surface. Using the same analysis method, the HAP-JF interface possesses a relatively weaker interfacial adhesion which requires an average of 1360 mN to fully expose the jute fiber surface. The MnO_2-CF interface suggests the lowest interfacial adhesion which only requires an average force of 946 mN for a full fiber-coating delamination. These results suggest implications for multifunctional applications of enhanced composites. Ultimately, our study provides a novel perspective for characterizing the interfacial adhesion in the nano-modified fiber reinforced composites and paves the way for future composite interface design for multifunctional composites.

Acknowledgments

This study was partially supported by NSF Advanced Manufacturing grant # 2001038, and the National Aeronautics & Space Administration through the University of Central Florida's NASA FLORIDA SPACE GRANT.

References

[1] Gibson, R.F., 2010. A review of recent research on mechanics of multifunctional composite materials and structures. Composite structures, 92(12), pp.2793-2810.

[2] Forintos, N. and Czigany, T., 2019. Multifunctional application of carbon fiber reinforced polymer composites: Electrical properties of the reinforcing carbon fibers–A short review. Composites Part B: Engineering, 162, pp.331-343.

[3] Mohammed, L., Ansari, M.N., Pua, G., Jawaid, M. and Islam, M.S., 2015. A review on natural fiber reinforced polymer composite and its applications. International journal of polymer science, 2015.

[4] Shah, S.Z.H., Karuppanan, S., Megat-Yusoff, P.S.M. and Sajid, Z., 2019. Impact resistance and damage tolerance of fiber reinforced composites: A review. Composite Structures, 217, pp.100-121.

[5] Kim, J.K. and Mai, Y.W. eds., 1998. Engineered interfaces in fiber reinforced composites. Elsevier.

[6] Zheng, H., Zhang, W., Li, B., Zhu, J., Wang, C., Song, G., Wu, G., Yang, X., Huang, Y. and Ma, L., 2022. Recent advances of interphases in carbon fiber-reinforced polymer composites: A review. Composites Part B: Engineering, 233, p.109639.

[7] Valadez-Gonzalez, A., Cervantes-Uc, J.M., Olayo, R.J.I.P. and Herrera-Franco, P.J., 1999. Effect of fiber surface treatment on the fiber–matrix bond strength of natural fiber reinforced composites. Composites Part B: Engineering, 30(3), pp.309-320.

[8] Chandra, N., and Namilae, S., "Tensile and compressive behavior of carbon nanotubes: Effect of functionalization and topological defects," Mechanics of Advanced Materials and Structures, vol. 13, Mar. 2006, pp. 115–127.

[9] Srihari, S., Sathyanath, R., Kalpathy, S. K., Al-Haik, M., and Namilae, S., "Effect of nanoscale surface modification on the interfacial mechanics of carbon fibers," Advanced Materials Interfaces, Sep. 2024.

[10] Wu, Y., Yang, Z., Madiyar, F., Jiang, Y., and Namilae, S., "Hydroxyapatite functionalized natural fiber-reinforced composites: Interfacial modification and Additive Manufacturing," Polymer Composites, Aug. 2024.

[11] Gholampour, A. and Ozbakkaloglu, T., 2020. A review of natural fiber composites: Properties, modification and processing techniques, characterization, applications. Journal of Materials Science, 55(3), pp.829-892.
[12] Ashraf, M.A., Peng, W., Zare, Y. and Rhee, K.Y., 2018. Effects of size and aggregation/agglomeration of nanoparticles on the interfacial/interphase properties and tensile strength of polymer nanocomposites. Nanoscale research letters, 13, pp.1-7.
[13] Marot, G., Lesage, J., Démarécaux, P., Hadad, M. and Staia, M.H., 2006. Interfacial indentation and shear tests to determine the adhesion of thermal spray coatings. Surface and Coatings Technology, 201(5), pp.2080-2085.
[14] Chicot, D., Démarécaux, P. and Lesage, J., 1996. Apparent interface toughness of substrate and coating couples from indentation tests. Thin solid films, 283(1-2), pp.151-157.
[15] Xie, Y., Zhang, X., Robertson, M., Maric, R. and Ghosh, D., 2006. Measurement of the interface adhesion of solid oxide fuel cells by indentation. Journal of power sources, 162(1), pp.436-443.
[16] Lin, Y., Ehlert, G., & Sodano, H. A. (2009). Increased interface strength in carbon fiber composites through a ZnO nanowire interphase. Advanced functional materials, 19(16), 2654-2660.
[17] Kumar, D., Dusabimana, M. C., Al-Haik, M., & Namilae, S. (2023). Effect of nanoscale interface modification on residual stress evolution during composite processing. Journal of Composite Materials, 57(19), 2995-3011.
[18] Shah, H.U., Wang, F., Javed, M.S., Ahmad, M.A., Saleem, M., Zhan, J., Khan, Z.U.H. and Li, Y., 2018. In-situ growth of MnO2 nanorods forest on carbon textile as efficient electrode material for supercapacitors. Journal of Energy Storage, 17, pp.318-326.
[19] Yu, H.P., Zhu, Y.J. and Lu, B.Q., 2018. Highly efficient and environmentally friendly microwave-assisted hydrothermal rapid synthesis of ultralong hydroxyapatite nanowires. Ceramics International, 44(11), pp.12352-12356.
[20] Tomastik, J. and Ctvrtlik, R., 2013. Nanoscratch test—A tool for evaluation of cohesive and adhesive properties of thin films and coatings. In EPJ web of conferences (Vol. 48, p. 00027). EDP Sciences.
[21] Jardret, V., Zahouani, H., Loubet, J.L. and Mathia, T.G., 1998. Understanding and quantification of elastic and plastic deformation during a scratch test. Wear, 218(1), pp.8-14.
[22] Perry, A.J., 1983. Scratch adhesion testing of hard coatings. Thin solid films, 107(2), pp.167-180.
[23] Sari, F. N., So, P., and Ting, J., "MnO2 with controlled phase for use in supercapacitors," Journal of the American Ceramic Society, vol. 100, Jan. 2017, pp. 1642–1652.